PREDICTION OF PULSATILE 3D FLOW IN ELASTIC TUBES USING STAR CCM+ CODE

D.P. de Andrade[*], J.M.C. Pereira AND J.C.F. Pereira

[*]Instituto Superior Técnico / Universidade de Lisboa, Mech. Eng. Depart. LASEF
Av. Rovisco Pais 1, 1049-001 Lisbon, Portugal
e-mail: didier.philippe.andrade@tecnico.ulisboa.pt

Key words: Pulsatile flow, Curved pipe, Dean flow, Lyne flow, Secondary flow, Collapsible tube flow, Fluid-structure interaction (FSI), Finite Volume Method

Abstract. Three-dimensional fluid-structure interaction is studied numerically in several elastic straight or curved pipes under a pulsatile flow. The finite volume code STAR-CCM+ is used to solve the fluid-structure interaction problem governed by the Navier Stokes equations with the large displacement model in a stongly coupled interaction. Two cases are considered for the validation purposes: straight collapsible tube with different thicknesses, for validation of the fluid-structure model and pulsatille flow in a rigid curved pipe. Finally, the comparison between rigid and elastic walls on the pulsatile flow in a curved pipe is performed for several Young modulus and Womersley numbers. The results show a detailed validation of the STAR-CCM+ code for the fluid-structure interaction model problem and a physical sound result considering the influence of the wall elasticity on the Dean vortices of the secondary flow.

1 INTRODUCTION

The study of periodic flows in the laminar regime is of particular interest in many engineering applications and particularly for blood flow in the physiological circulation. These flows are characterized by a function of velocity or pressure which varies in time. A pulsatile flow is a periodic flow that oscillates around a mean value which is not equal to zero.

The studies concerning oscillatory and pulsatile flows go as far back as the 1950's. It is thanks to these first analytical studies that, for a fully developed regime, the fundamental characteristic parameters of the flow were determined. In oscillating flow the interaction between viscous and inertial effects originates a deviation of the velocity profile from the parabolic shape of a steady flow [19, 18, 1].

When studying steady laminar flow through ducts, even the slightest curvature has an effect on the flow which is non-negligible. These effects originate from the centrifugal force

which induces a pressure gradient and secondary flows. The secondary flow consists in a pair of counter-rotating symmetrical cortices known as Dean cells [5, 6], which appear in the duct cross-section. Steady fully developed laminar Newtonian curved flows of circular cross-section have been studied extensively, [2] presented some of the previous work.

For a critical value of Dean number a second pair of counter-rotating vortices appear, called hereafter Dean vortices, on the outer (concave) wall of the pipe. These vortices come from the Dean instability which belong to the large family of centrifugal instabilities to which the Taylor-Couette and Görtler instabilities also belong to.

[10] highlighted the complexity of the fully developed laminar oscillatory flow in curved pipes. Continuing the work of Dean [5, 6] he introduced a flow generated by a pressure gradient varying sinusoidally around zero and demonstrated the appearance of a new vortex pair over and above those observed in the steady case. Theoretical confirmation of these results was made by [20] and experimentally by [3] Lyne vortices appear with an increase in the frequency parameter in a pulsating curved duct flow. The secondary flow in a curved pipe depends on the Womersley parameter, Reynolds number and Dean number.

In the cardiovascular field the pulsatory flow is of particular interest for blood circulation and vascular ageing. Some of the works done in this field were done by [12, 14, 7]. [13] observed in an analytical study of pulsatile flows in curved pipes, with a strong curvature radius, that the amplitude of shearing forces decreases with increasing frequency. Also, considerable variation in the secondary flow intensity occurs at small frequencies of oscillation during a pulsation cycle.

[15] made several experimental measurements of the axial and secondary velocities in a 180° curved pipe. They highlighted the presence of reverse flows at the inside wall during the deceleration phase. The reverse flows and the appearance of the cortex were highlighted numerically by [17], confirmed the presence of more than two vortex pairs in the secondary flow. [4] found that the secondary flow had only one vortex pair at the beginning of the deceleration process. When at half-phase of deceleration, the secondary flow becomes more complex with the formation of a new vortex pair near the outside wall that disappears when the last third of the deceleration phase begins, only to reappear at the end of the acceleration process. [8, 9] studied the effect of Reynolds number on pulsatile flow and concluded that the secondary flow increases in complexity with an increase of the stationary Reynolds number.

There is an incredible richness in the flow in curved pipes. Previous studies have studied the influence of the parameters that affect the secondary flow. However very few works have concentrated on the implications of having an elastic tube. The main purpose of this study is to compare the secondary flow development under rigid and elastic pipe curvature.

2 Numerical Model

The CFD commercial software STAR-CCM+ is used to solve the unsteady Navier-Stokes equations and the solid mechanics.

2.1 Equations: Solid Mechanics

The process by which the wall deformation is calculated is done according to the following steps. Taking the differential form of the solid momentum equation:

$$\rho \ddot{u} = \bigtriangledown \bullet \sigma + b \tag{1}$$

where b is the body force, and a general constitutive law between the stress tensor and the strain tensor:

$$\sigma = \sigma(\varepsilon, T, k) \tag{2}$$

where T is the temperature and k represents other internal variables. Also since small strain is assumed we can use $\varepsilon = \frac{1}{2}(\bigtriangledown U + \bigtriangledown U^T)$ to characterize strain. The finite volume form is now determined by the integration of parts to obtain:

$$\int\limits_V \rho \ddot{u} dV = \int\limits_A \sigma dA + \int\limits_V b dV \tag{3}$$

The acceleration terms can be modelled either using a 1st order (Backward Euler) or a 2nd order (Newmark). In STAR-CCM+ the large displacement model is also included since the displacement can be as large as the cell size.

During a numerical simulation where the structural behaviour is analysed, there can be a lack of either physically real or unwanted numerical damping. To try and solve this problem the Rayleigh Damping methodology is used. The damping is written as:

$$C = \frac{M}{\tau_M} + \tau_K K \tag{4}$$

where C is the viscous damping matrix, M is the mass matrix, K is the stiffness matrix, $\frac{1}{\tau_M}$ is the mass damping coefficient, and τ_K is the stiffness damping coefficient. In the finite volume stress analysis the stiffness matrix is not computed, instead an equivalent law for viscous stress is used:

$$\sigma_d = 2G\dot{\varepsilon} + \lambda tr(\dot{\varepsilon})\delta \tag{5}$$

where $\dot{\varepsilon}$ is the rate of change of the deformation rate gradient. The total stress is given as the sum of the elastic and viscous damping parts and with an elastic model with pseudo strain of the form:

$$\tilde{\varepsilon} = \varepsilon + \tau_K \dot{\varepsilon} \tag{6}$$

the elastic model returns the total stress due to both the elastic and viscous damping.

2.2 Equations: Fluid Model

The fluids used during the simulation can be assumed as incompressible, under such hypothesis the Navier-Stokes equations are given as:

$$\frac{\partial \rho}{\partial t} + \frac{\partial \rho U}{\partial x} = 0 \tag{7}$$

$$\frac{\partial U}{\partial t} + u \bullet \bigtriangledown U = -\frac{\bigtriangledown P}{\rho} + \nu \bigtriangledown^2 u \tag{8}$$

where ν is the kinematic viscosity, U is the velocity of the fluid, P is the pressure and ρ is the fluid density. The Eq.(13) is known as the continuity equation and Eq.(14) as the momentum equation.

Since the fluid is viscous and incompressible, the following constitutive equation is used:

$$\tau_{ij} = 2\mu s_{ij} \tag{9}$$

which relates the stress tensor τ_{ij} and the strain rate tensor s_{ij}, μ is the dynamic viscosity of the fluid. The strain rate tensor is defined as:

$$s_{ij} = \frac{1}{2}\left(\frac{\partial U_i}{\partial x_j} + \frac{\partial U_j}{\partial x_i}\right) \tag{10}$$

The solving methodology is done with a segregated solver which can be described as using a collocated variable arrangement and a Rhie-andChow-type pressure-velocity coupling combined with a SIMPLE-type algorithm. For boundary conditions the no slip condition is applied at the wall.

A pulsated flow of velocity pulsation ω is then characterized by the following parameters:

- the Womersley number $\alpha = r_0(\omega/\nu)^{1/2}$, also known as the frequency parameter,

- the Reynolds number $R_e = (U * D_h)/\nu$, which for the oscillating flow we take the maximum velocity, $U_{max,osc}$, and for the steady flow we take the mean velocity $U_{m,st}$,

- the Dean number $D_n = \frac{U_m D_h}{\nu}\sqrt{\frac{D_h}{R_c}}$ where U_m is the mean velocity, ν is the kinematic viscosity, D_h is the hydraulic diameter and R_c is the mean radius of curvature.

- the ratio $\beta = U_{max,osc}/U_{m,st}$, which characterizes the balance between the steady and oscillating components of the pulsated flow,

- the oscillating velocity amplitude, defined in a flow cross-section as: $U_{osc} = U_{max,osc} * \sin(\omega t) = [\frac{1}{\pi r^2}\int_0^R 2\pi r U(r)dr]\sin(\omega t)$.

3 Validation of the Fluid/Structure

Two benchmarks are used to validate the software: a three-dimensional straight collapsible tube and a rigid curved pipe. The first is a numerical solution while the second has both numerical and experimental.

3.1 Straight Collapsible Tube

Table 1 lists the main parameters of test case 1.

Table 1: Summary of case from [11]

Case	1	2
Solid Properties		
Radius (R)	4 [mm]	4 [mm]
Length (L_{up})	R	R
Length ($L = L_{down}$)	10R	10R
Thickness	$\frac{R}{20}$	$\frac{2R}{20}$
Density	2702 [Kg/m^3]	[Kg/m^3]
Young Modulus	3 [MPa]	3 [MPa]
Poisson Coefficient	0.3	0.3
Fluid Properties		
Reynolds number	350	350
Physical conditions		
Pressure	520 [Pa]	1550 [Pa]
Rayleigh Damping		
Mass damping coefficient	-4.73944 [Hz]	-10.0338 [Hz]
Stiffness damping coefficient	8.84E-4 [s]	8.58 [s]

The main objective is to obtain a degree of collapse of 86.4% of the radius. The error obtained with the thinner mesh refinement was of 0.32% for the thin tube and of 0.18% for the thick tube. The error for the location of maximum collapse was well under 3% for both cases. Thus the results obtained are considered to be in good agreement.

3.2 Flow through a $90°$ Rigid Curved Pipe

Table 2 lists the main parameters of the test case 2.

The main results are to observe the development of the secondary flow and the velocity profiles along the axial axes on the 90° section of the pipe. Several meshes were used in order to assess mesh convergence. A mesh with close to 500.000 cells is required to achieve convergence and a low margin of error. A sketch of the geometry is shown in Figure 1.

Figure 2 and Figure 3 show the comparison between the experiments and the present predictions. The velocity profiles are in good agreement with the experiment and also the details of the secondary flow are shown in Figure 4.

The evolution of the secondary flow is explained in part with the frequency parameter which can be defined as the ratio between the inertial forces due to the local acceleration and the viscous forces determining the movement over a time scale which is equivalent to the oscillation period. A lower Womersley number ($\alpha \leq 1$) will either imply a large

Table 2: Summary of case from [16]

Case	1	2
Solid Properties		
Radius (R)	0.02 [mm]	0.02 [mm]
Length (L_{up})	2.5 [m]	2.5 [m]
Length (L_{out})	0.5 [m]	0.5 [m]
Radius curvature	0.22 [m]	0.22 [m]
Fluid Properties		
Reynolds number steady	600	600
Womersley number	12.14	17.17
Velocity ratio β	1	1
Density	1000 [Kg/m^3]	1000 [Kg/m^3]
Dynamic viscosity	0.001 [Pa-s]	0.001 [Pa-s]

viscous layer near the wall, a large oscillation period compared to the viscous layer near the wall or a large oscillation period in comparison to the viscous diffusion time. When in the presence of this situation the secondary flow field will be similar to that obtained in a curved pipe with a stationary flow over the whole pulsation cycle. If however there is an increase in the Womersley number then, as expected, not only the secondary flow intensity increases but also the viscosity effect is confined to the wall region and the inertial effects increase in the central area of the section. This disequilibrium of the forces increases the effects of the centrifugal force in the cross-section centre; in the close proximity of the external wall, the tangential velocity is larger than the radial velocity and fluid particles which were close to the flow centre will start to move towards the external wall. the vortices formed at this stage will gradually stretch, and their centres will begin to move slightly to the top and bottom of the section in a symmetrical way. The axial velocity presents an annular form with a peak near the wall which coincides with the velocity at the vortex centres and a valley in the cross-section centre. The reason for the rising of the valley is due to the fluid no longer obeying the axial pressure gradient variation, in the central area, in comparison to the fluid which is close to the wall.

With even greater increase in the Womersley number the fluid close to the concave wall causes the secondary flow to stop and a stagnation zone appears close to the concave wall. The pressure gradient becomes more predominant than the centrifugal force in the section centre and in some occasions, the fluid present in the stagnation region and in the vicinity of the concave wall initiate a rotational movement. Near to the wall an additional pair of vortices are created and will occupy the section centre and in the same time will push the centre of the other vortices to the top and bottom of the tube cross-section. When the secondary flow presents such a configuration, with four counter rotating vortices, it is called the Lyne instability. This instability has a very complex formation process since it involves an alteration of the balance of the centrifugal force, pressure gradient and the inertial force.

One cannot however characterize the Lyne vortices by the Womersley number uniquely. Has expected the Reynolds number also plays an important role. For instance, if a low Reynolds number is used then the secondary flow presents only the two Dean cells, which

have a low intensity in relation to higher Reynolds numbers. In the presence of a large Reynolds number a maximum of the velocity radial distribution is found near the concave wall.

Another parameter that influences the Lyne vortices is the amplitude ratio defined as β. If this value is under the unity then a quasi-stationary flow appears. This is due to the dominance of the stationary component on the oscillating component and the velocity field distribution does not depend on the Womersley number (α). With a velocity amplitude equal to unity then the velocity field becomes more complicated and an annular region begins to appear. The secondary flow thus can present some particularly interesting fields depending on the Womersley number.

During the deceleration phase of a pulsated flow, if the stationary component is not too large in comparison to the time-dependent component, the fluid movement near the wall presents a reversed flow in relation to the flow in the centre of the section centre. This reverse flow increases near the convex wall. Close to the wall one can observe that the shear stress varies not only in magnitude but also in direction.

4 Results

4.1 Flow through a $90°$ Elastic Curved Pipe

With the validation completed it is now necessary to repeat the analysis with an elastic pipe. The elastic tube is applied on the curved section only. Table (3) presents the properties of the solid used.

Table 3: Summary of Solid Parameters

Case	
Solid Properties	
Thickness	2.32 [mm]
Density	2702 [Kg/m^3]
Young Modulus 1	3 [MPa]
Young Modulus 2	0.0625 [MPa]
Poisson Coefficient	0.3
Rayleigh Damping	
Mass damping coefficient (Young Modulus 1)	-0.33996 [Hz]
Stiffness damping coefficient (Young Modulus 1)	0.004018 [s]
Mass damping coefficient (Young Modulus 2)	-0.04907 [Hz]
Stiffness damping coefficient (Young Modulus 2)	0.002784 [s]

Table (4) presents the maximum wall displacement in relation to tube thickness obtained in the elastic pipe.

Table 4: Maximum Displacement in relation to tube thickness

	Young Modulus 1	Young Modulus 1
Womersley number = 12.14	0.05 [%]	2.32 [%]
Womersley number = 17.17	0.08 [%]	4.22 [%]

The elastic wall influences the flow through the deformation that contributes to the pressure gradient to become even more predominant than in the rigid case.

For the lower Womersley number case the velocity profile obtained with the elastic pipe shows very small deviations to the one obtained with the rigid pipe. Only in the 270° phase there is some difference. This is somewhat to be expected since the wall displacement is very low. However with the second case the velocity profile exhibits large differences when the less rigid tube is used. The margin of difference goes as high as 25%. It is also important to stress that this is obtained with a mere 4.22% maximum displacement in relation to wall thickness. The difference in wall shear stress can be seen at 0 radians and at π radians.

REFERENCES

[1] Atabek, H.B., Chang, C.C., *Oscillatory flow near the entry of a circular tube, Zamp.* (1961) **12**:403-422.

[2] Berger, S.A., Talbot, L., Yao, L.S., *Flow in curved pipes, Ann. Rev. Fluid Mech.* (1983) 461-512.

[3] Bertelsen, A.F., *An experimental investigation of low Reynolds number secondary streaming effects associated with an oscillating viscous flow in a curved pipe, Int. J. Fluid Mech.* (1975) **(part 3) 70**:519-527.

[4] Chang, L.J., Tarbell, J.M., *Numerical simulation of fully developed sinusoidal and pulsatile (physiological) flow in curved tubes, J. Fluid Mech.* (1985) **161**:175-198.

[5] Dean, W.R., *Note on the motion of fluid in a curved pipe, Philos. Mag. J. Sci.* (1927) **4**:208-223.

[6] Dean, W.R., *The streamline motion of fluid in a curved pipe, Philos. Mag. J. Sci.* (1928) **5**:673-695.

[7] Deplano, V., Siouffi, M., *Experimental and numerical study of pulsatile flows through stenosis: wall shear stress analysis, J. Biomech.* (1999) **32**:1081-1090.

[8] Hamakiotes, C.C., Berger, S.A., *Fully developed pulsatile flow in a curved pipe, J. Fluid Mech.* (1988) **195**:23-55.

[9] Hamakiotes, C.C., Berger, S.A., *Periodic flow through curved tubes: the effect of the frequency parameter, J. Fluid Mech.* (1990) **210**:353-370.

[10] Lyne, W.H., *Unsteady viscous flow in a curved pipe, J. Fluid Mech.* (1971) **(part 1) 45**:13-31.

[11] Marzo, A.,Luo X.Y.,Bertram C.D.,*Three-dimensional collapse and steady flow in thick-walled flexible tubes, Journal of Fluids and Structures* (2005) **20**:817-835.

[12] Pedley, T.J., *The fluid mechanics of large blood vessels Cambridge Monogr. Mech. Appl. Mathe.* (1980) 160-224.

[13] Rabadi, N.J., Simon, M.A., Chow, J.C.F., *Numerical solution for fully developed, laminar pulsating flow in curved tubes*, Numer. Heat Transfer (1980) **3**:225-239.

[14] Siouffi, M., Deplano, V., Pelissier, R., *Experimental analysis of unsteady flows a stenosis*, J. Biomech. (1998) **31**:11-19.

[15] Talbot, L., Gong, K.O., *Pulsatile entrance flow in a curved pipe*, J. Fluid Mech. (1983) **127**:1-25.

[16] Timité B., Castelain C., Peerhossaini H., *Pulsatile viscous flow in a curved pipe: Effects of pulsation on the development of secondary flow*, International Journal of Heat and Fluid Flow (2010) **31**:879-896.

[17] Toshihiro, T., Kouzou, S., Masaru, S., *Pulsating flow in curved pipes 1:numerical and approximate analysis*, Bull. JSME 27 (1984) **234**:2706-2713.

[18] Uchida, S., *The Pulsating Viscous Flow Superposed on the Steady Laminar Motion of Incompressible Fluid in a Circular Pipe*, Institute of Science and Technology, University of Tokyo (1956) **7**:403-422.

[19] Womersley, J.R.,*Oscillatory motion of a viscous liquid in a thin walled elastic tube I: the linear approximation for long waves*, J. Physiol. (1954). 199-221.

[20] Zalosh, R.G., Nelson, W.G., *Pulsating flow in a curved tube*, J. Fluid. Mech. (1973) **59**693-705.
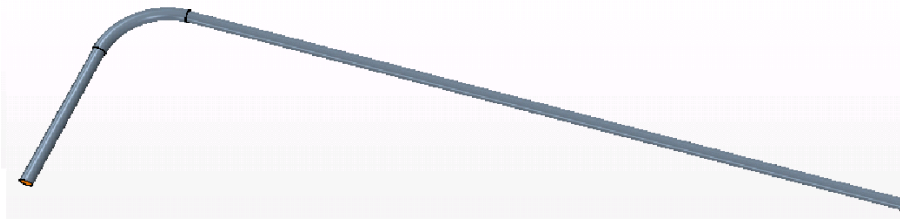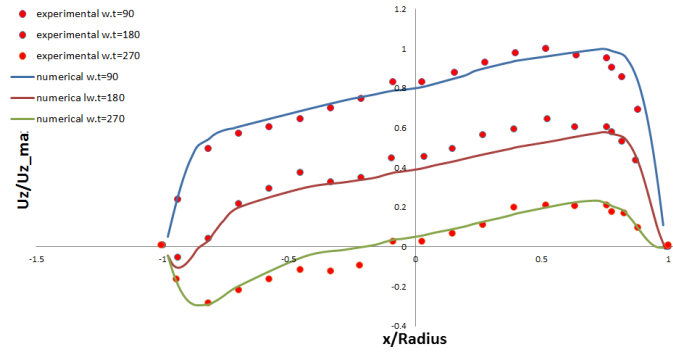
Figure 1: Tube Geometry

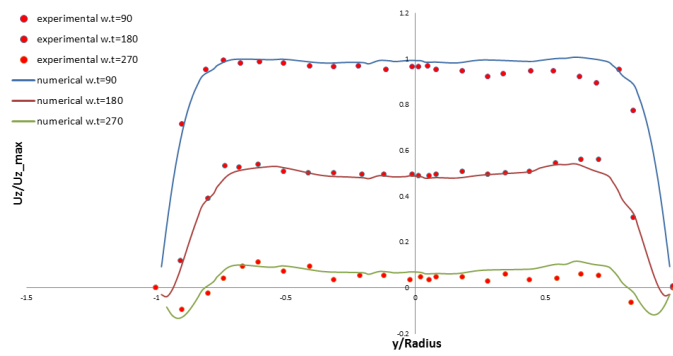Figure 2: Velocity Profile x for Womersely 12.14

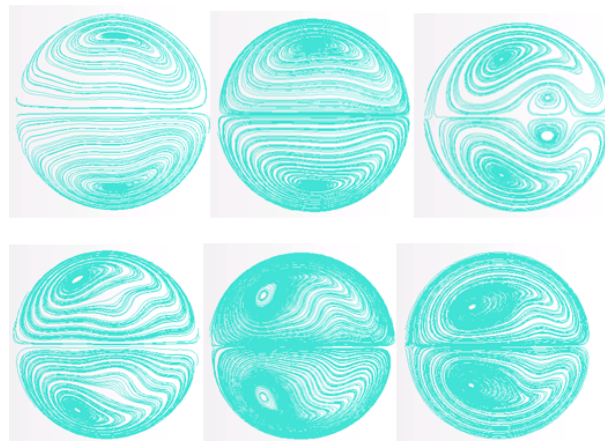Figure 3: Velocity Profile y for Womersely 12.14

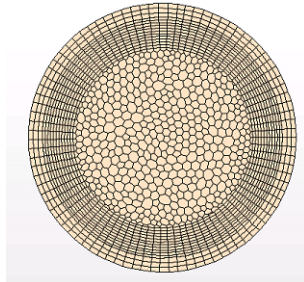Figure 4: Secondary Flow for Womersley 17.17 and 12.14
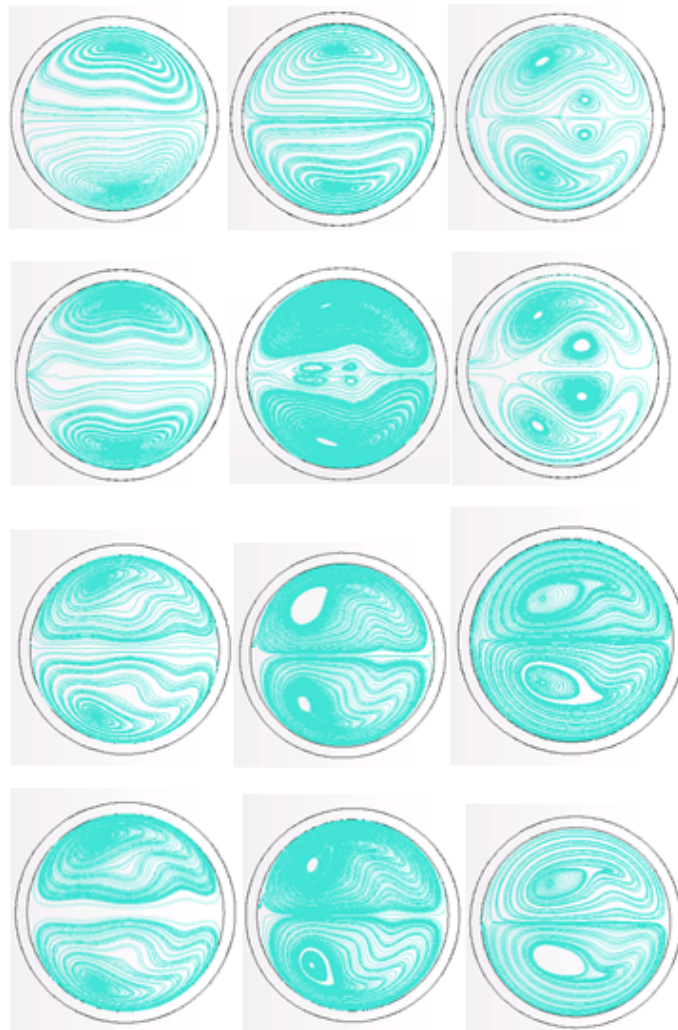
Figure 5: Mesh

Figure 6: Secondary flow for Young Modulus 1 and 2, the first two rows are for Womersley=17.17 and the other two rows for Womersley=12.14.
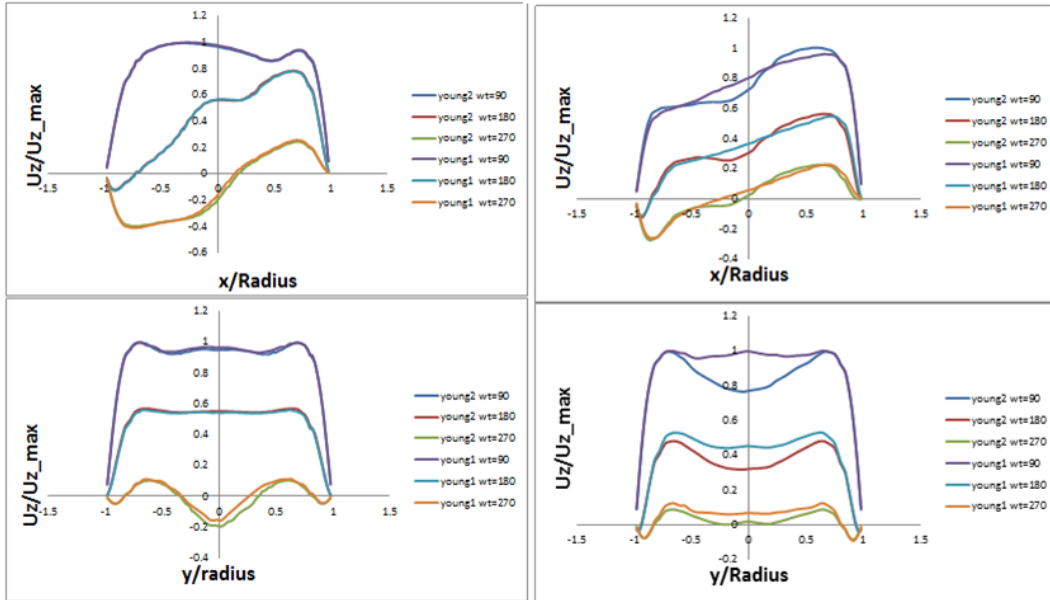
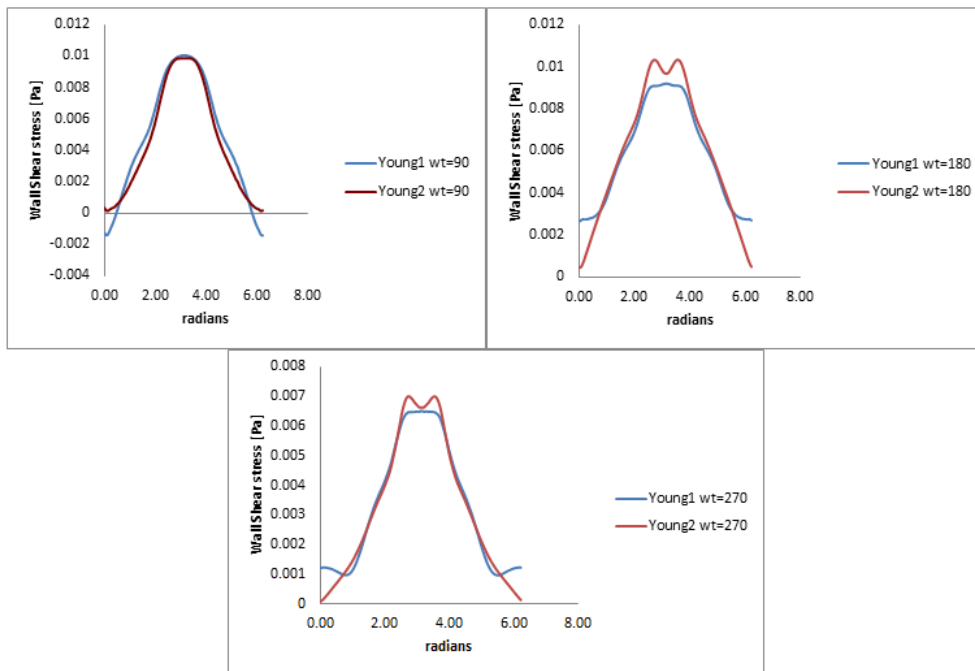Figure 7: Velocity profiles left column Womersley 12.14, right column Womersley 12.14.

Figure 8: Wall Shear Stress for Womersley=17.17.